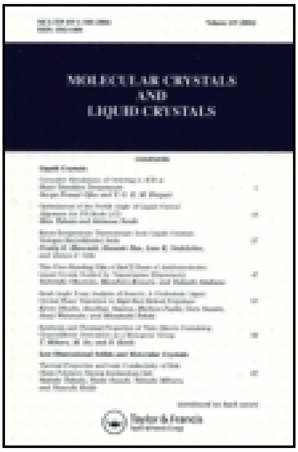

Molecular Crystals and Liquid Crystals
Publication details, including instructions for authors and subscription information:
http://www.tandfonline.com/loi/gmcl20

Infrared Spectra of Charge Transfer Complexes of Biocytin With Organic Acceptors

Ashvin Padhiyar [a], A. J. Patel [a] & A. T. Oza [a]

[a] Department of Physics, Sardar Patel University, Vallabh Vidyanagar, Gujarat, India

To cite this article: Ashvin Padhiyar, A. J. Patel & A. T. Oza (2012): Infrared Spectra of Charge Transfer Complexes of Biocytin With Organic Acceptors, Molecular Crystals and Liquid Crystals, 552:1, 228-246

To link to this article: http://dx.doi.org/10.1080/15421406.2011.604268

Mol. Cryst. Liq. Cryst., Vol. 552: pp. 228–246, 2012
Copyright © Taylor & Francis Group, LLC
ISSN: 1542-1406 print/1563-5287 online
DOI: 10.1080/15421406.2011.604268

Infrared Spectra of Charge Transfer Complexes of Biocytin With Organic Acceptors

ASHVIN PADHIYAR, A. J. PATEL, AND A. T. OZA*

Department of Physics, Sardar Patel University, Vallabh Vidyanagar,
Gujarat, India

The infrared (IR) spectra of the well-known biomolecules called biocytin and their charge transfer complexes with standard organic acceptors such as TCNQ (7,7,8,8-tetracyano-p-quinodimethane), TCNE (tetracyano-p-ethylene), DDQ (2,3- dichloro-5,6-dicyano-p-benzoquinone), chloranil, and iodine have been studied in the present work. The spectrum of biocytin contains a beta density at high frequency and a slightly asymmetric triangular distribution as well as a U-shaped distribution at low frequency, the latter being associated with anisotropic disorder. Weak charge transfer from TCNE and iodine reduces the width of U-shaped distribution and makes the triangular peak more asymmetric. Strong CT interactions with TCNQ and DDQ make the triangular peak in absorption become a Gaussian distribution. The strongest interaction with chloranil leads to oscillations in the density of states with square-root singularities. Toward the high frequency side, the interband transition do occur but with either spin-orbit splitting or exciton-phonon coupling. There is correlated hopping in biocytin-iodine complex.

Keywords Charge transfer interaction; gaussian distribution; spin-orbit splitting; triangular distribution; U-shaped distribution

PACs 71.20NE; 78.30JW; 87.15Mi.

Introduction

Long chain biomolecules like fatty acids, β-carotene, tripalmitin etc. are well known [1]. Biocytin, the active form of biotin, also known as biotinyllysine residue is also a long chain biomolecule. Polypeptide chain of enzyme is attached to a lysine residue that in turn is attached to a biotin molecule [1]. The reactive group is a double five membered ring containing two NH groups and one sulfur atom with two C–S bonds, which makes biocytin a donor molecule. The spectra of iodine complexes of fatty acids and tripalmitin were studied recently [2]. In the present work, we study the FTIR spectra of biocytin and its charge transfer complexes with standard electron acceptors like chloranil, DDQ, TCNQ, TCNE, and iodine. The molecular structure of biocytin is shown in Fig. 1.

---

*Address correspondence to A. T. Oza, Department of Physics, Sardar Patel University, Vallabh Vidyanagar, Gujarat, India. E-mail: ajayozat@yahoo.com

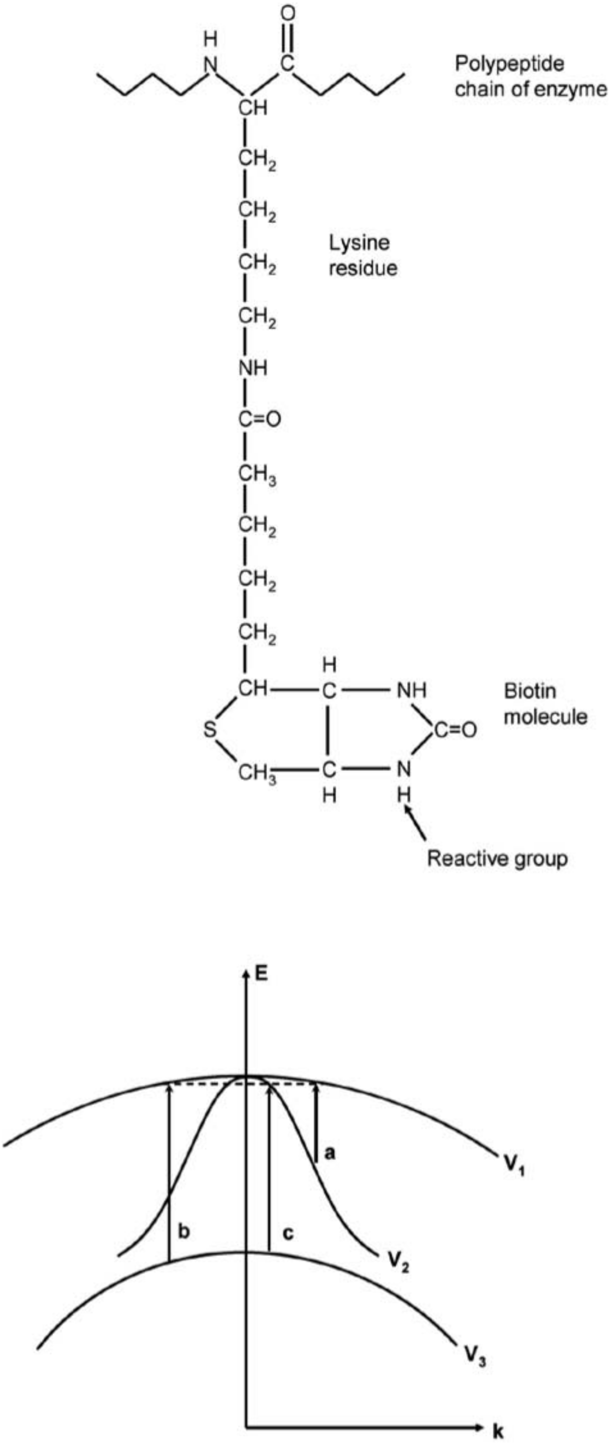

Figure 1. Molecular structures and spin-orbit splitting of valence band of biocytin.

Experimental

Biocytin, in powder form, was obtained from Aldrich Chemical Company as an analytical reagent grade. Organic acceptors like chloranil, DDQ (2,3- dichloro-5,6-dicyano-p-benzoquinone), TCNQ (7,7,8,8-tetracyano-p-quinodimethane), TCNE (tetracyano-p-ethylene), and iodine obtained from standard chemical companies with high purities were mixed one by one with biocytin in 1:1 molecular weight proportions. The mixtures were taken in agate mortar and were ground until homogeneous mixtures were obtained and colors changed remarkably. The powders of Charge Transfer Complexes (CTCs) thus obtained were further mixed with spectrograde dry KBr powder and ground until 5% of the complexes dispersed in 95% KBr powder. Palates of circular shape were prepared in a compressor machine with a dye that was manually operated. The semitransparent disks prepared this way were placed in the dark sample chamber of standard spectrophotometer of Perkin Elmer Co., USA. The FTIR spectra were recorded in the range of 400 cm^{-1} to 4000 cm^{-1} of wave numbers.

Results and Discussion

The FTIR spectrum of biocytin in the full IR range is shown in Fig. 2. This mainly contains five regions:

(1) Above 2200 cm^{-1} with a few vibrational bands riding over a half power beta density peak, the later showing hoping of charge carriers across a large inter molecular distance.
(2) Between 1700 cm^{-1} and 2200 cm^{-1} revealing a transmitting range without pronounced absorption peaks.

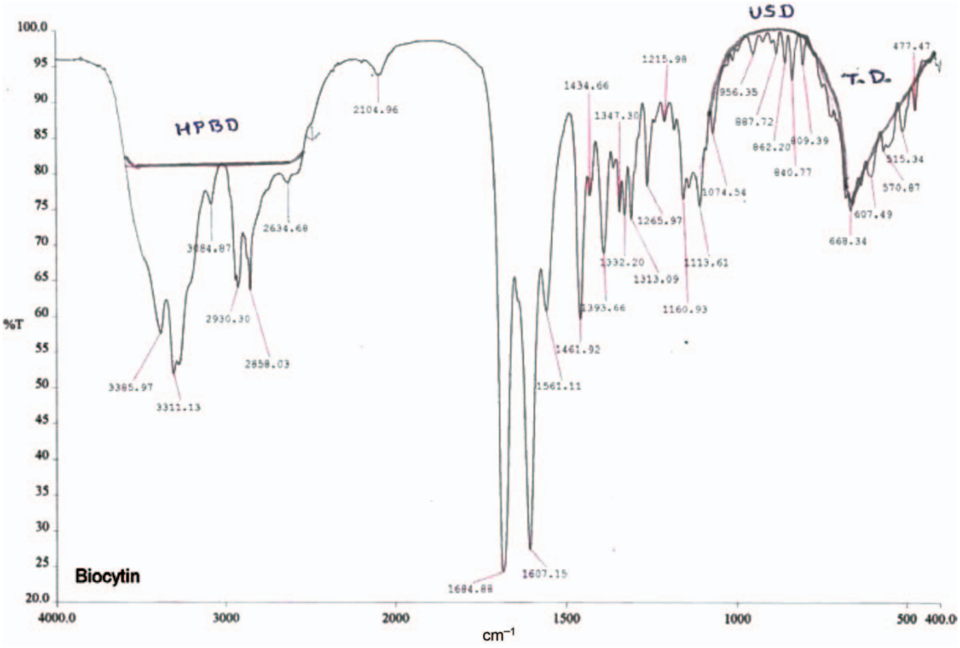

Figure 2. Infrared (IR) spectrum of biocytin (Color figure available online).

Table 1. IR spectrum of biocytin

Shape of the envelope or background absorption	Range of the absorption profile	FWHM (cm^{-1} and in eV)
Half-power beta density	3800–2400 cm^{-1}	1000 cm^{-1} (0.125 eV)
Transmission range	2400–1750 cm^{-1}	—
Vibrational structures	1750–1100 cm^{-1}	—
U-shaped distribution	1100–670 cm^{-1}	375 cm^{-1} (0.047 eV)
Triangular distribution	750–400 cm^{-1}	185 cm^{-1} (0.023 eV)

(3) Between 1050 cm^{-1} and 1700 cm^{-1} having a large number of vibrational and rotational bands.

(4) Between 900 cm^{-1} and 1050 cm^{-1} containing a U-shaped distribution in absorption.

(5) Below 900 cm^{-1} containing a triangular distribution steeply rising below 900 cm^{-1} and slowly falling below 600 cm^{-1} and hence being asymmetric. The results are summarized in Table 1.

The U-shaped distribution arises out of preferential alignment of biocytin molecules along its long direction. When there is a random 3D orientation of molecules that are almost neutral, there is semicircular distribution in absorption in the lower IR range. This is observed in CTCs of neutral amino acid called tryptophan. When the molecule has a long chain in one direction, there is parallel or anti-parallel arrangement in one direction with little angle among the molecules. This type of anisotropy in molecular peaking in a microcrystallite can lead to U-shaped distribution rather then a semicircular distribution in isotropic materials. U-shaped distribution is known in statistics. Thus, there is an anisotropic disorder of biocytin molecule.

Another interpretation arises out of the density of states in 1D alloys. If the probability of finding a charge carrier on A and B type atoms randomly arranged across a line, that is, $P_{\text{A}} = P_{\text{B}}$, this gives rise to semicircular plot in the graph of the density of states $D|E|$ vs. energy E. If $P_{\text{A}} = 0.05$ and $P_{\text{B}} = 0.95$, that is, when there is a large difference between probabilities, there is U-shaped distribution [3]. This 1D alloy model can also explain U-shaped distribution found in the spectrum of biocytin.

Finally, a triangular distribution is found around 600 cm^{-1}, which is also asymmetric, can be explained with the tilting of band edges forming a triangular barrier in the presence of internal electric field [4]. A rectangular potential barrier of the forbidden energy band gap becomes triangular barrier because of slant valence and conduction bands allowing tunneling of charge carriers. The tunneling probability is higher for a triangular potential barrier by two orders of magnitude than that in the case of rectangular potential barrier [5]. Thus, there is internal Franz–Keldysh effect also called Redshift effect. The electromagnetic absorption tracks the triangular barrier in the present case. This shows that there is strong electric field probably related with the dipole moment of biocytin molecule. There is parallel and anti-parallel arrangement of these dipole moments.

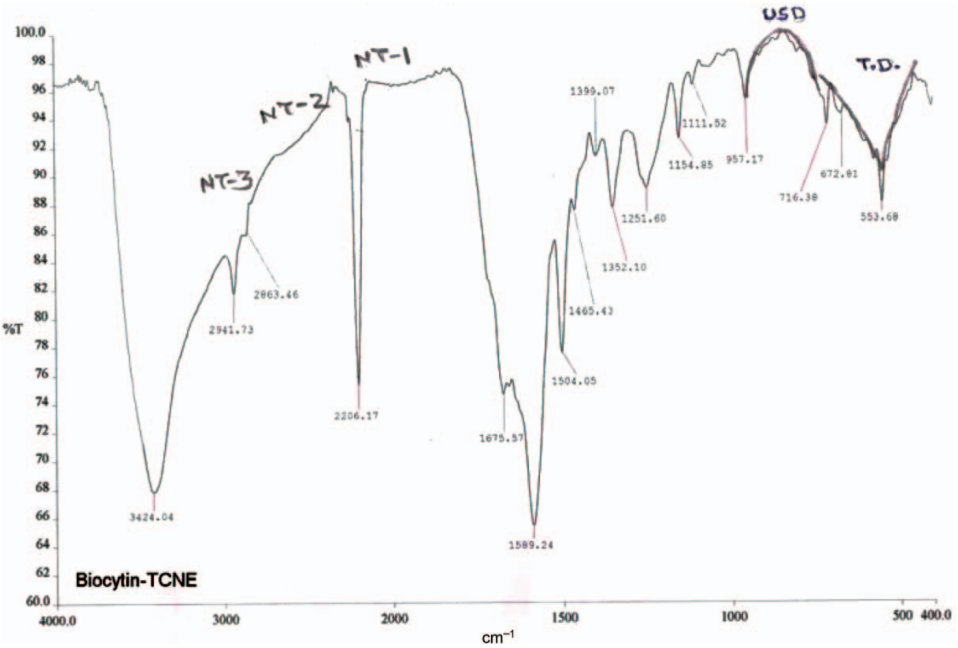

Figure 3. IR spectrum of biocytin-TCNE complex (Color figure available online).

The spectrum of biocytin-TCNE complex is shown in Fig. 3. This spectrum can also be divided into five regions:

(1) Above 3000 cm^{-1} where a broad and intense band is observed at 3424 cm^{-1}.
(2) Between 1750 cm^{-1} and 3000 cm^{-1} where three transitions marked as NT-1, NT-2, and NT-3 are observed.
(3) Between 1000 cm^{-1} and 1750 cm^{-1} having a large number of vibrational and rotational bands.
(4) Between 716 cm^{-1} and 1000 cm^{-1} containing a U-shaped distribution having somewhat narrow absorption dip than in the biocytin spectrum.
(5) Between 400 cm^{-1} and 700 cm^{-1} containing a triangular distribution but steeply rising above 400 cm^{-1} and slowly falling toward 700 cm^{-1}, thus, oppositely asymmetric as compared to that in the spectrum of only biocytin. The results are summarized in Table 2.

The three transitions observed between 1750 cm^{-1} and 3000 cm^{-1} are associated with the transitions between the three valance sub bands and conduction band. The three valance sub bands can arise from the spin orbit splitting of the valance band in to three sub bands [6–8]. When the top of the valence band is populated with holes, it is possible to make three types of photon absorbing transitions among the sub bands. The absorption is proportional to hole density [9,10]. Rather than these intraband transitions, we observe a transition from each sub band to a conduction band in the IR range, in the present case. The subband transitions $V_3 \rightarrow V_1$, $V_3 \rightarrow V_2$, and $V_2 \rightarrow V_1$ are described elsewhere [4]. The transitions are directly detected [11,12]. The differences between absorption edges (Eg) are noted in Table 3.

Table 2. IR spectra of biocytin-TCNE and biocytin-iodine

Shape of the envelope or background absorption	Range of the absorption profile		FWHM (cm^{-1} and in eV)	
	TCNE complex	Iodine complex	TCNE complex	Iodine complex
Broad and intense absorption band	3800–2950 cm^{-1}	3700–2930 cm^{-1}	580 cm^{-1} (0.0725 eV)	480 cm^{-1} (0.06 eV)
Interband transitions	2860–1800 cm^{-1}	2930–1800 cm^{-1}	—	—
Vibrational structures	1800–1000 cm^{-1}	1800–1000 cm^{-1}	—	—
U-shaped distribution	957–673 cm^{-1}	950–720 cm^{-1}	170 cm^{-1} (0.0213 eV)	120 cm^{-1} (0.0125 eV)
Triangular distribution	672–450 cm^{-1}	670–450 cm^{-1}	140 cm^{-1} (0.0175 eV)	00 cm^{-1} (0.0125 eV)

Table 3. A-Nature of transitions (NT) in biocytin complexes

Name of complex	NT-1 Abs. function	Eg (eV)	NT-2 Abs. function	Eg (eV)	NT-3 Abs. function	Eg (eV)
Biocytin-TCNE	$\alpha h\nu = A(h\nu - E_g)^{3/2}$	0.23eV	$\alpha h\nu = A(h\nu - E_g)^2$	0.33eV	$\alpha = A(h\nu - E_g)^2$	0.34eV
Biocytin-iodine	$\alpha h\nu = A(h\nu - E_g)^{1/2}$	0.225eV	$\alpha h\nu = A(h\nu - E_g)^{1/2}$	0.275eV	$\alpha = A(h\nu - E_g)^3$	0.33eV
Biocytin-TCNQ	$\alpha h\nu = A(h\nu - E_g)^3$	0.216eV	$\alpha h\nu = A(h\nu - E_g)^3$	0.284eV	$\alpha = A(h\nu - E_g)^3$	0.318eV
Biocytin-DDQ	$\alpha h\nu = A(h\nu - E_g)^3$	0.23eV	$\alpha h\nu = A(h\nu - E_g)^{1/2}$	0.296eV	$\alpha = A(h\nu - E_g)^3$	0.34eV
Biocytin-chloranil	$\alpha h\nu = A(h\nu - E_g)^{3/2}$	0.22eV	—	—	—	—

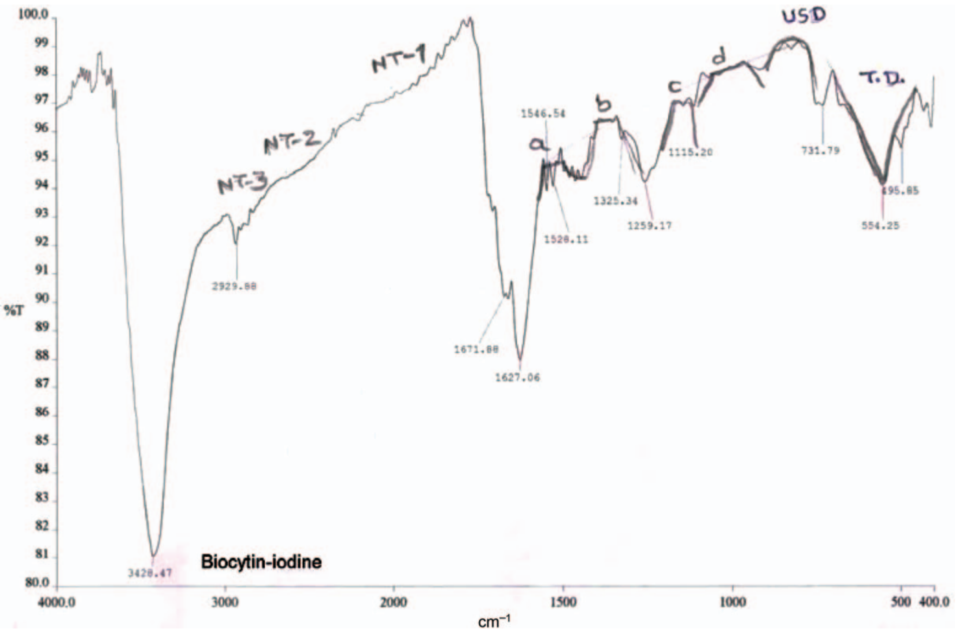

Figure 4. IR spectrum of biocytin-iodine complex (Color figure available online).

The U-shaped distribution observed around 835 cm^{-1} in biocytin-TCNE spectrum is assigned to the narrowed U-distribution in biocytin alone due to change in electron-phonon interaction and charge transfer from biocytin to TCNE. TCNE withdraws charges from two N-H groups and two C–S bonds of the biocytin molecule. The narrowing of U-shaped distribution suggests increase in anisotropy due to charge transfer. In biocytin-TCNE complex, biocytin molecules are partially positively charged leading to increase in dipole moment. The increase in dipole–dipole interaction leads to increase in anisotropic alignment.

The spectrum of biocytin-iodine complex is also shown in Fig. 4. The intermolecular interaction between donor and acceptor molecules is stronger than that in the TCNE complex. The spectrum again can be divided into five parts:

(1) Above 3000 cm^{-1} containing a broad and intense absorption band.
(2) Between 1700 cm^{-1} and 3000 cm^{-1} containing three transitions marked as NT-1, NT-2, and NT-3. The absorption functions are somewhat different as compared to TCNE complex (Table 4).
(3) Between 1000 cm^{-1} and 1750 cm^{-1} this time consisting a cascade of four half-power beta density (flat peaks in transmission) peaks in the spectrum marked as a, b, c, and d.
(4) A narrow U-shaped distribution in the range of 730 cm^{-1} to 1000 $\mathrm{cm}^{-1,}$ which is narrower than that for the TCNE complex revealing stronger charge transfer interaction.
(5) A triangular distribution between 400 cm^{-1} and 730 cm^{-1}, which is slightly asymmetric.

Table 4. B-Intraband transitions

Complex	Transition	ΔE
Biocytin-TCNE	$V_3 \rightarrow V_1$	0.11eV
	$V_3 \rightarrow V_2$	0.01eV
	$V_2 \rightarrow V_1$	0.1eV
Biocytin-iodine	$V_3 \rightarrow V_1$	0.105eV
	$V_3 \rightarrow V_2$	0.055eV
	$V_2 \rightarrow V_1$	0.05eV
Biocytin-TCNQ	$V_3 \rightarrow V_1$	0.102eV
	$V_3 \rightarrow V_2$	0.024eV
	$V_2 \rightarrow V_1$	0.078eV
Biocytin-DDQ	$V_3 \rightarrow V_1$	0.11eV
	$V_3 \rightarrow V_2$	0.044eV
	$V_2 \rightarrow V_1$	0.066eV

The special feature of biocytin-iodine spectrum is the observation of four flat peaks in the region of vibrational and rotational bands. These flat peaks are half-power beta densities obeying

$$T = T_0 + T_1 K^{*1/2}(1 - K)^{*1/2}$$

Where $K^* = (K - a)/b$. These types of series of beta density peaks were observed in the UV-Visible spectra of the CTCs of lead phthalocyanine [13]. There were absorption peaks lowering in intensity as energy increased. Here also the peaks are decreasing in intensity as energy increases. But, the peaks are in transmission rather than absorption. This series of beta densities can be attributed to a correlated hopping, which is phonon assisted. The fact that these kinds of peaks are not found in any other biocytin complex in the present work suggests that the hopping occurs along iodine chains in biocytin-iodine complex.

The equation of energy level for particle in a rectangular well is given by [14],

$$2E^{1/z}(V_0 - E)^{1/z} \cos\left[(2mE)^{1/z}\frac{e}{\hbar}\right]$$

The amplitude $E^{1/Z}(V_0 - E)^{1/Z}$ is nothing but the flat half-power beta density peak and $\cos[(2mE)^{1/Z}\frac{e}{\hbar}]$ shows repetition of such a structure. Thus, iodine chain provides a series of rectangular well for a charge carrier residing and moving along it.

The spectrum of biocytin-TCNQ complex is shown in Fig. 5. The charge transfer interaction is stronger and of different type as understood from this spectrum. The spectrum has four distinct regions:

(1) Above 2900 cm^{-1} having a fine structure of few vibrational and rotational bands retained from spectrum of biocytin alone.
(2) Between 1750 cm^{-1} and 2950 cm^{-1} containing three transitions corresponding to spin-orbit splitting of valence band.

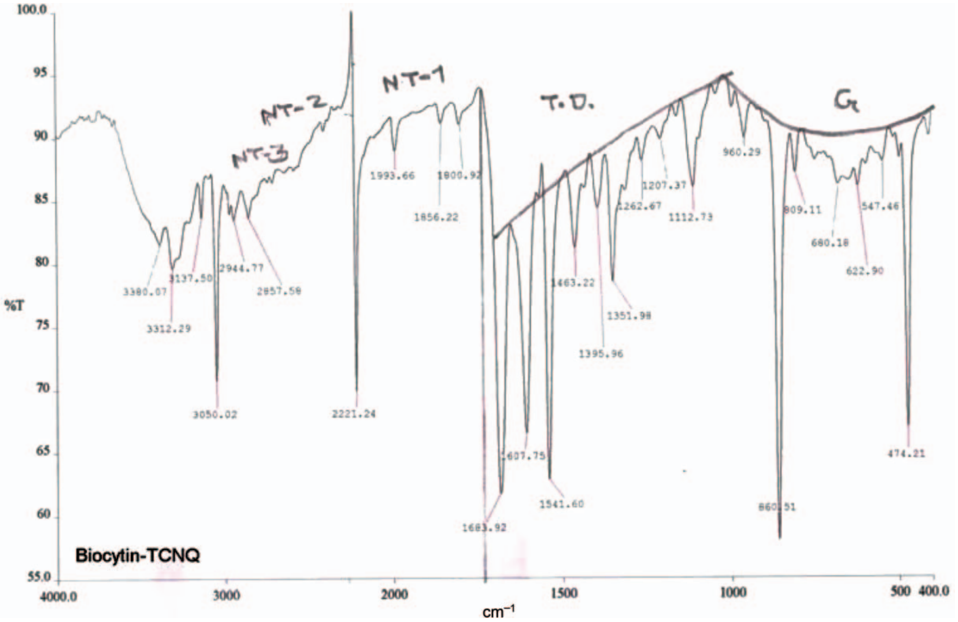

Figure 5. IR spectrum of biocytin-TCNQ complex (Color figure available online).

(3) A region of asymmetric triangular distribution between 1000 cm^{-1} and 1750 cm^{-1} in background absorption, and
(4) A broad Gaussian absorption peak between 400 cm^{-1} and 1000 cm^{-1}. These results are also summarized in Table 5.

The triangular background absorption between 1000 cm^{-1} and 1750 cm^{-1} is asymmetric having steep rise below 1750 cm^{-1} and falling below 1650 cm^{-1}. The peak is nearly (not exactly) triangular and shows a shape corresponding to screening function related to imperfect nesting [15]. This feature is also found in biocytin-DDQ along with a Gaussian function in the lower region. The charge transfer occurs from the whole of TCNQ or DDQ molecule having reversible and negative half-wave reduction polarographic potential and not only from the end-groups as in TCNE complex. NT-1 transition in TCNQ complex reveals an absorption function appropriate for a layered or 2D material. Gaussian distribution in the lower range below 1000 cm^{-1} reveals an intermediate behavior between metal and semiconductor. For a metal, a Cauchy distribution is followed due to the Drude model and for a semiconductor, a Lorentzian profile is followed for the Lorentz model of damped-driven oscillator [16]. Gaussian distribution is derivable from these two extremes as having an intermediate band width or the full-width at half-maximum.

The spectrum of biocytin-DDQ is also displayed in Fig. 6. This also has four regions:

(1) Above 2900 cm^{-1} having a few vibrational and rotational bands.
(2) Between 1750 cm^{-1} and 2900 cm^{-1}, having three transitions corresponding to spin-orbit split valence band.
(3) A triangular background absorption between 900 cm^{-1} and 1750 cm^{-1} as arising from the imperfect nesting of the Fermi surface.

Table 5. IR spectra of biocytin-TCNQ and biocytin-DDQ

Shape of the envelope or background absorption	Range of the absorption profile		FWHM (cm^{-1} and in eV)	
	TCNQ complex	DDQ complex	TCNQ complex	DDQ complex
Gaussian background	3800–2400 cm^{-1}	—	1200 cm^{-1} (0.15 eV)	—
Oscillator model	—	3800–2300 cm^{-1}	—	750 cm^{-1} (0.094 eV)
Interband transitions	2900–1750 cm^{-1}	2850–1800 cm^{-1}	—	—
Vibrational structure and background asymmetric triangular distribution	1650–1000 cm^{-1}	1660–990 cm^{-1}	500 cm^{-1} (0.0625 eV)	430 cm^{-1} (0.054 eV)
Gaussian distribution	1000–400 cm^{-1}	850–400 cm^{-1}	360 cm^{-1} (0.045 eV)	250 cm^{-1} (0.0313 eV)

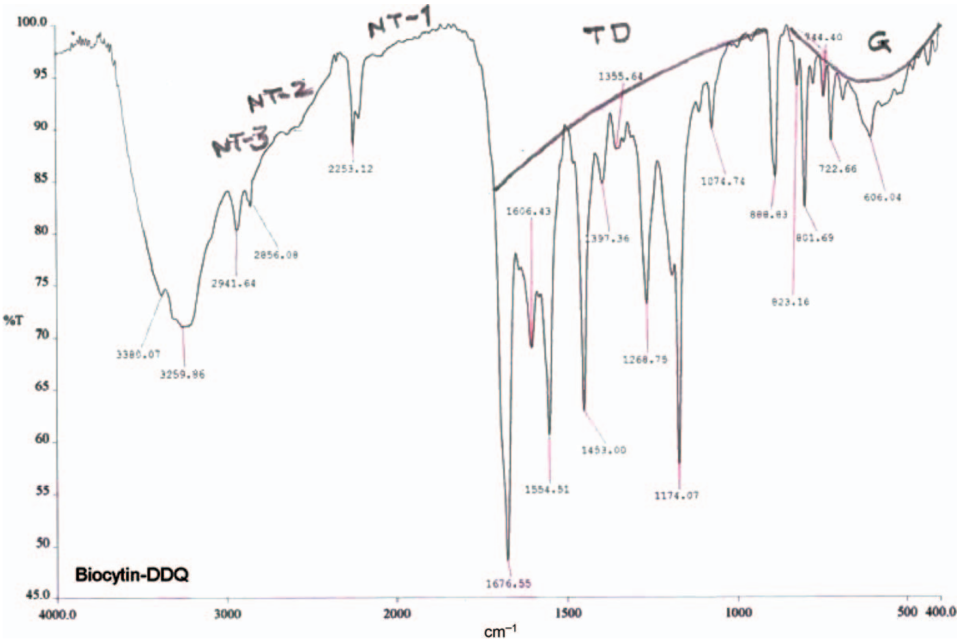

Figure 6. IR spectrum of biocytin-DDQ complex (Color figure available online).

(4) Between 400 cm^{-1} and 850 cm^{-1} containing a somewhat narrower Gaussian band than that in TCNQ complex.

The nature of transitions in the spin-orbit splitting region shows that two out of three (NT-1 and NT-2) transitions follow $\alpha h\nu = A(h\nu - E_g)$, which is the absorption function for 2D (layered) materials. Thus, biocytin-DDQ is a layered material. It is more layered than TCNQ complex of biocytin. The Gaussian background absorption band in the lowest region reveals weaker electron-phonon coupling than the TCNQ complex, because the full-width at half-maximum of the Gaussian peak is proportional to the electron-phonon coupling constant.

The last spectrum of biocytin-chloranil is shown in Fig. 7. Here, the charge transfer interaction is maximum smearing out the splitting of the valence band due to spin-orbit interaction. As a result, only one transition from valence band to conduction band is observed as usually observed in binary CTCs. The highest range above 1830 cm^{-1} contains only a broad absorption band. Between 400 cm^{-1} and 1750 cm^{-1} (below 1750 cm^{-1}), there are oscillations of the background absorption arising from the oscillations in the density of states corresponding to the 1D vibrations of a monoatomic or a homomolecular lattice. This shows that there are segregated stacks as observed in strongly interacting systems and the motions in 1D give rise to square-root singularities. The transverse effects dominate because such behavior of the oscillations in the density of states as found in the presence of magnetic field [17]. The results are summarized in Table 6.

On the other hand, the repeated structures of the square-root singularities can be compared with an astable multivibrator. Both the shapes of the peaks and the repetition

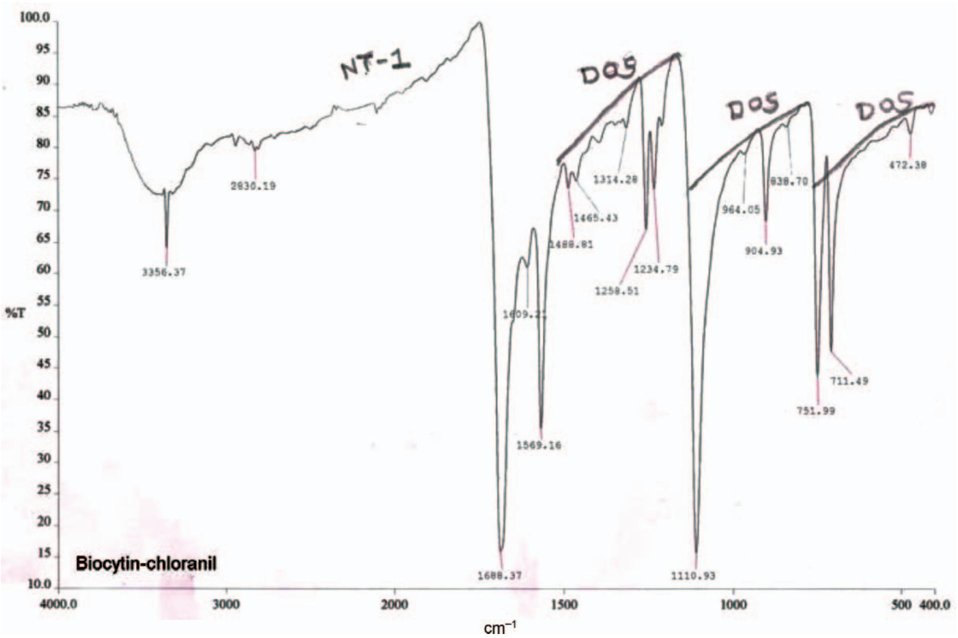

Figure 7. IR spectrum of biocytin-chloranil complex (Color figure available online).

are identical in these two physical systems. Acridine-orange-TCNQ and acridine-orange-TCNE show similar repeated structures, which were described as molecular multivibrators [18]. The system vibrates several times due to quasi-stable screening and imperfect nesting. Thus, biocytin-chloranil is a molecular multivibrator and is more 1D conductor rather than 2D or 3D conductor. The absorption functions for the three absorption edges marked as NT-1, NT-2, and NT-3 in the absorption spectra are fitted (Figs 8–12). The results are summarized in Table 3.

Table 6. IR spectrum of biocytin-chloranil

Shape of the envelope or background absorption	Range of the absorption	FWHM* (cm^{-1} and in eV)
Oscillator model	3800–3000 cm^{-1} (3360 cm^{-1})	300 cm^{-1} (0.0375 eV)
Interband transition	2830–180 cm^{-1}	—
Vibrational structures	1800–400 cm^{-1}	—
Singularity position of the oscillations of the density of states	1690 cm^{-1} (First) 1110 cm^{-1} (Second) 750 cm^{-1} (Third)	450 cm^{-1} (0.056 eV) 160 cm^{-1} (0.02 eV) 80 cm^{-1} (0.01 eV)

*Full width at half maximum.

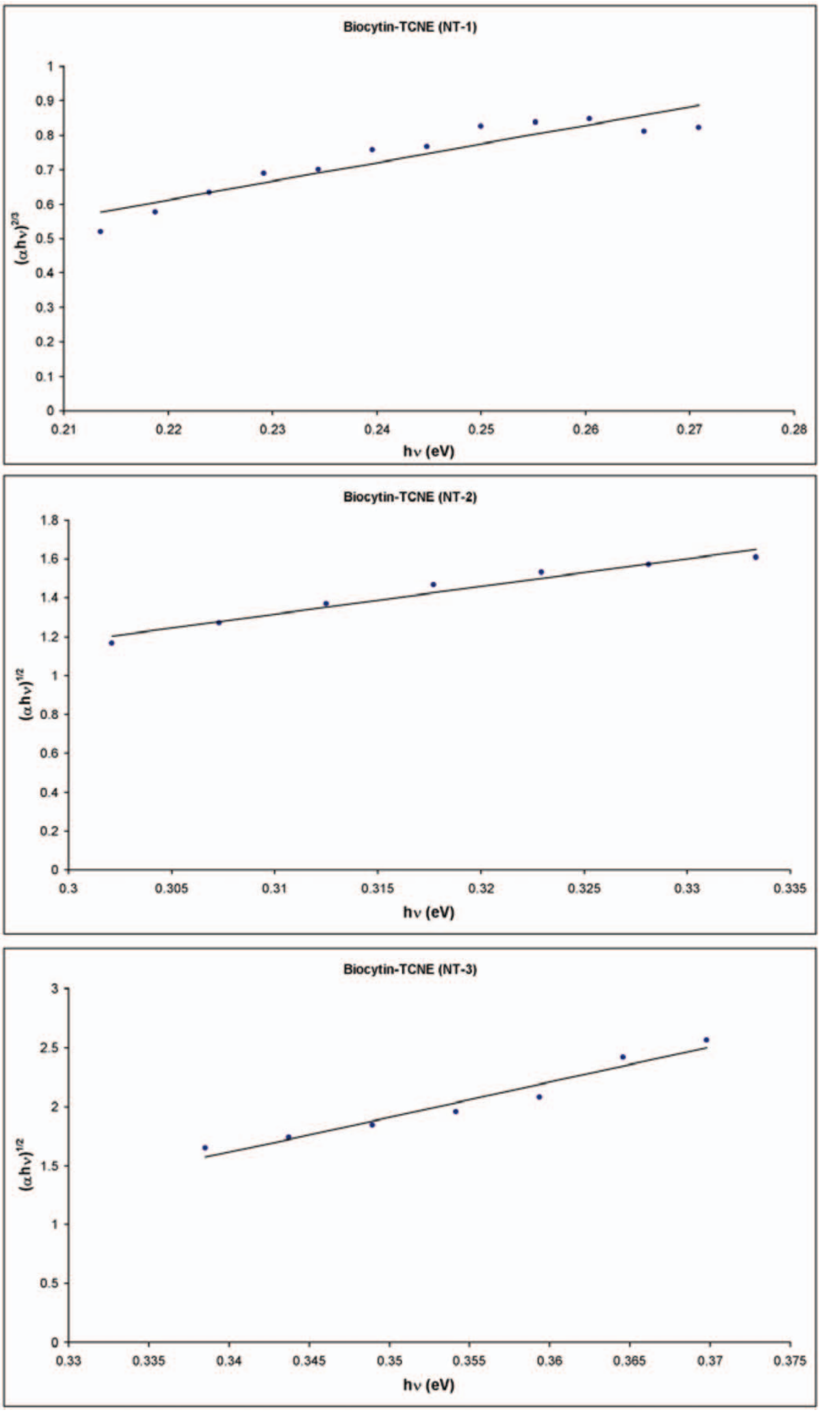

Figure 8. Three transitions in biocytin-TCNE complex (Color figure available online).

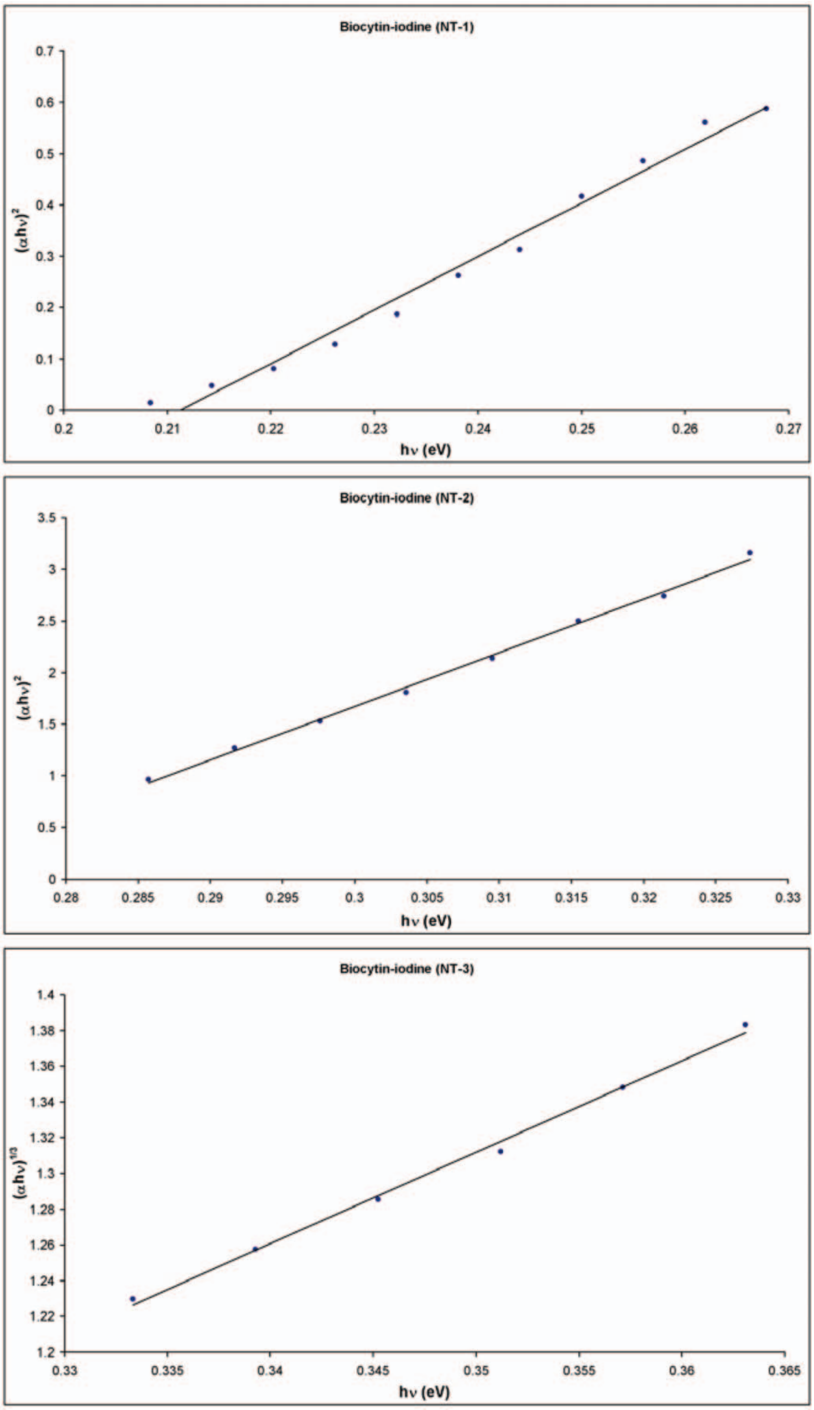

Figure 9. Three transitions in biocytin-iodine complex (Color figure available online).

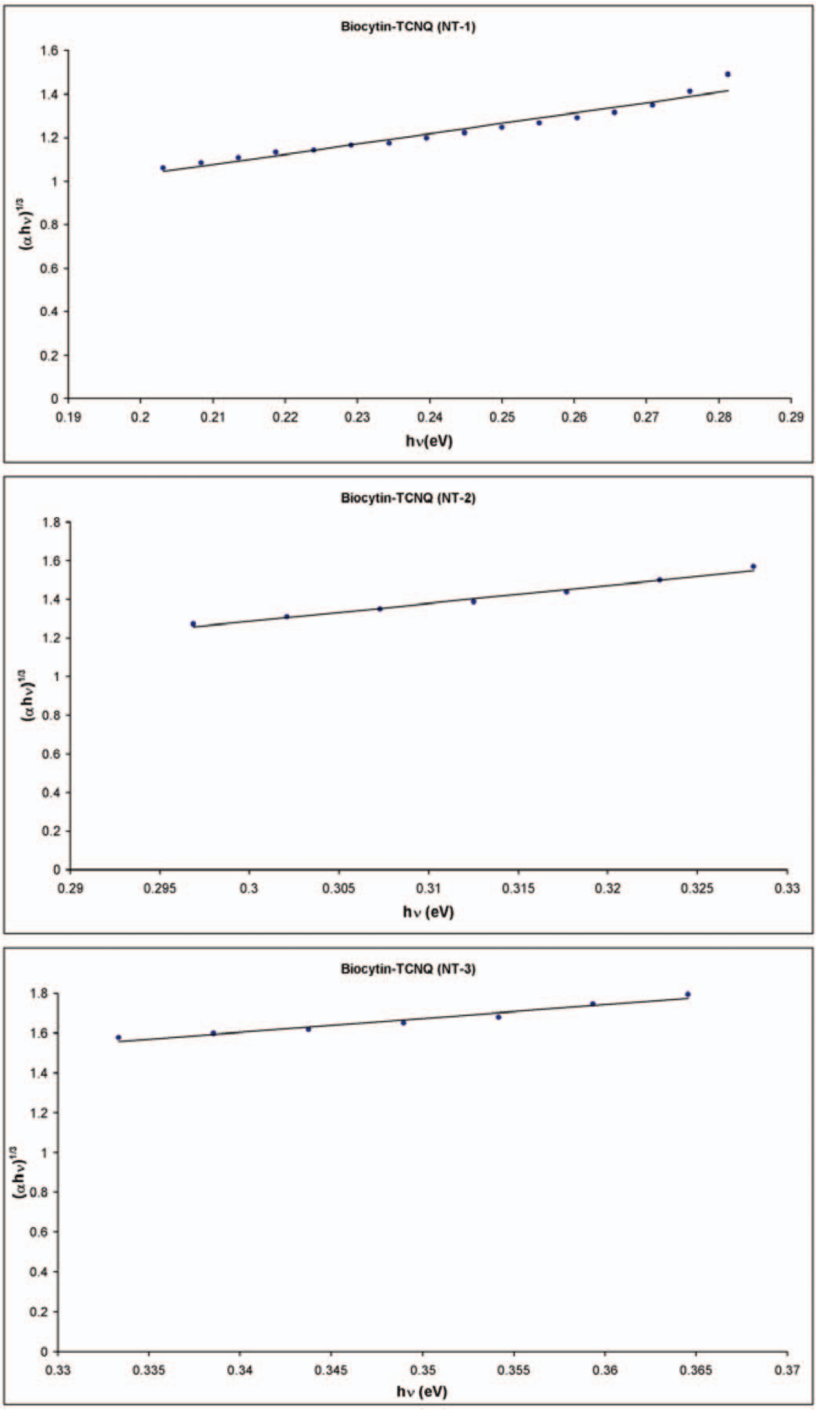

Figure 10. Three transitions in biocytin-TCNQ complex (Color figure available online).

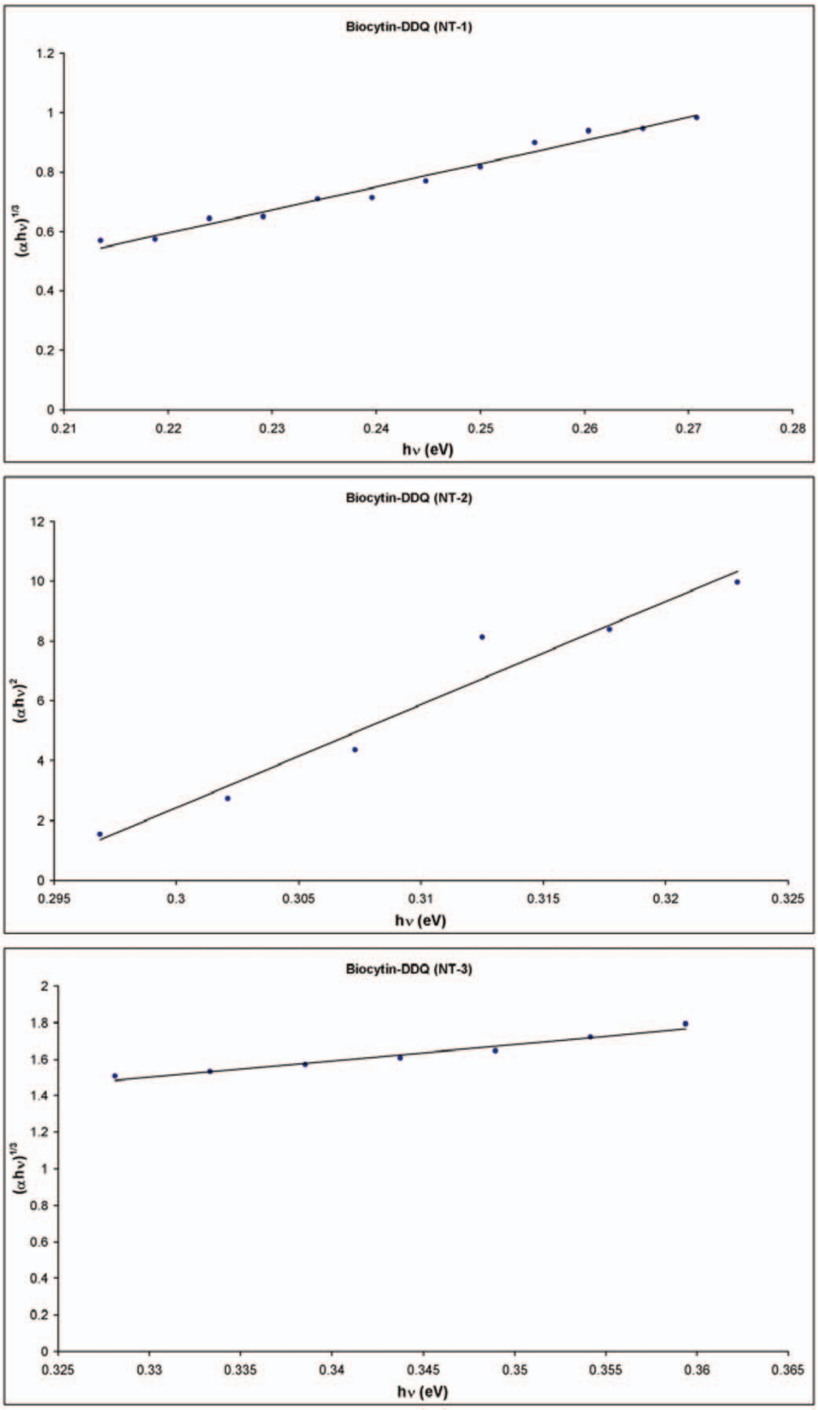

Figure 11. Three transitions in biocytin-DDQ complex (Color figure available online).

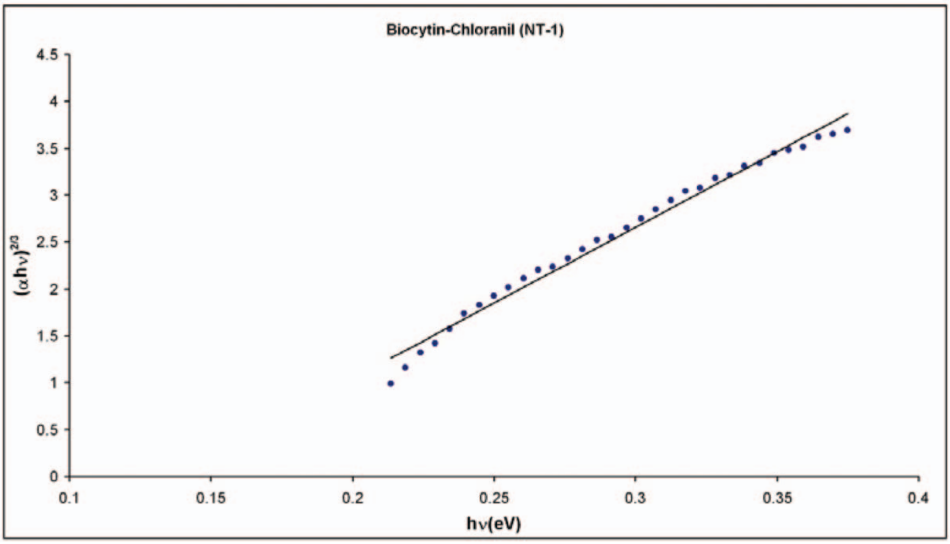

Figure 12. Transition in biocytin-chloranil complex (Color figure available online).

Conclusions

The spectra of biocytin complexes with organic acceptors reveal spin-orbit splitting of valence band when the charge transfer interactions are weak or intermediate. The spectrum of biocytin-chloranil shows oscillations in the density of states corresponding to square-root singularities for motions in 1D. TCNQ and DDQ complexes are layered materials.

References

[1] Lehninger, A. L. (1984). *Principles of Biochemistry*, CBS Publishers: Delhi.
[2] Ashvin B. Padhiyar, & Oza, A. T. (2003). *Prajna-SPU Res. Jour.*, *12*, 105.
[3] Plischke, M., & Bergersen, B. (1989). *Equilibrium Statistical Physics*, Prentice-Hall Inc. Englewood Cliffs, NJ. Edition, p. 297.
[4] Pankov, J. I. *Optical Processes in Semiconductors*, Prentice-Hall Inc.: Englewood Cliffs, NJ, p. 47.
[5] Gutmann, F., & Lyons, L. E. (1967). *Organic Semiconductors*, John Wiley and Sons Inc.: New York, p. 432.
[6] Herman, F., & Callaway, J. (1953). *Phys. Rev.*, *89*, 518.
[7] Dresselhans, G., Kip, A. F., & Kittel, C. (1954). *Phys. Rev.*, *95*, 568.
[8] Kaiser, W., Collins, R. J., & Fan, H. Y. (1953). *Phys. Rev.*, *91*, 1380.
[9] Briggs, H. B., & Fletcher, R. C. (1952). *Phys. Rev.*, *87*, 1130.
[10] Briggs, H. B., & Fletcher, R. C. (1952). *Phys. Rev.*, *91*, 1342.
[11] Kane, E. O. (1986). *J. Phys. Chem. Solids*, *1*, 82.
[12] Braunstein, R., & Kane, E. O. (1962). *J. Phy. Chem. Solids*, *23*, 1423.
[13] Prajapati, S. M., Oza, A. T., Navin Talpada, & Patel, R. G. (1999). *Prajna-SPU Res. Jour.*, *9*, 51.
[14] Ira N. Levine. (2000). *Quantum Chemistry*, 5th edn. Pearson Education Inc. Delhi, India. p. 30.

[15] Dora, B., Maki, K., & Virotztek, A. (2002). *Phys. Rev. B*, *66*, 165116.

[16] Dressel, M., & Grüner, G. (2002). *Electrodynamics of Solid*, Cambridge University Press: Cambridge, UK.

[17] Roth, L. M., & Argyres, P. N. (1966). In: R. K. Willardson & A. C. Beer (Eds.), *Seiconductors and Semimetals*, Vol. 1. Academic Press, p. 159.

[18] Agravat, S., Jain, V., & Oza, A. T. (2008). *Ind. J. Chem.*, *47A*, 341.